Bandpass Antenna-Filter-Antenna Arrays for Millimeter-Wave Filtering Applications

Hamza Kaouach[1,2,*] · Amar Kabashi[1,2] · Mohammed T. Simsim[1]

Abstract

This paper introduces new wideband antenna-filter-antenna (AFA) uniform arrays that can be utilized as frequency selective surfaces (FSS) with low loss and sharp roll-off response, which are highly desirable characteristics for millimeter wave applications. The design adopts a simple 3-layer single polarization structure consisting of two patch antennas and a resonator. Both simulations and measurements are used to characterize the performances of the proposed design. Overall results show 18.5% 10-dB bandwidth. For the targeted band the insertion loss is less than 0.2 dB. Possible applications include quasi-optical amps, grid mixers and radomes for aircraft radar antennas.

Key Words: Antenna-Filter-Antenna, Bandpass Filter Antenna, Frequency-Selective-Surfaces, Gaussian Optics Measurement System.

I. INTRODUCTION

An antenna-filter-antenna (AFA) element is composed of a receive antenna, a non-radiating resonant structure, and a transmit antenna operating between the input and output radiation ports [1]. These elements can be used for designing transmit-arrays (TA), when structured in a non-uniform array configuration [2]. They may also be used for designing frequency selective surfaces (FSS) when structured in a uniform array configuration [3]. The FSS can be viewed as filters with radiative ports, which are generally realized using planar periodic structures. Depending on the geometry, a single-layer FSS can present a bandpass or band-stop response around its resonant frequency.

In general, these elements are formed as three layer metallic structures: two resonant type planar antennas in the top and bottom layers, and one or more planar transmission line or slot resonators in the middle layer. Using AFA elements in the transmit-arrays results in a bandpass transfer function whose characteristics are desirable for radar, satellite [4], and power combining applications [5], where the distributed nature of the transmit-arrays can improve the power-handling and heat dissipation in the structure.

High-order filters are commonly designed using multi-layer FSS structures [6, 7]. Since the computational complexity drastically increases for multiple layers, the design of high-order frequency selective surfaces is performed by combining the individually designed FSS layers. The FSS layers, acting as individual resonators, are stacked using thick (0.2–0.3 λ_0) dielectric slab spacers which can be considered as simple impedance inverters, to form multi-pole filters. However, there are several problems with this method. First, the resulting filter topology as a chain of resonators and inverters is suitable only for a limited class of filter responses, which reduces the design space considerably. Second, the direct near-field coupling between the FSS layers in the stack and the loading effect of the dielectric

slabs can invalidate the simple resonator-inverter interpretation. As a result, the filter synthesis methods offer only a rough first-pass design, and the design procedure generally has to be followed by re-tuning the individual FSS layers and dielectric slabs using elaborate optimization methods. Third, the overall stacked structure can be thick and bulky which is not desirable for many applications.

This paper introduces a new approach to the AFA element design as a simple three-layer structure consisting of two patch antennas and co-planar waveguide (CPW) resonators. In contrast to the conventional stacked FSS designs, a higher order response can be achieved by simply adding resonators in the CPW layer, instead of increasing the number of layers, which simplifies the design significantly. The paper also demonstrates the measurement method used to extract the focusing *S*-parameters of the AFA element by utilizing a specially modified Gaussian optics measurement system. In addition to design simplicity, the obtained results show further attractive characteristics of the proposed element in terms of bandwidth, frequency response and overall efficiency.

The rest of the paper is organized as follows. In Sections II and III, we introduce the concept and design of the AFA element. The measurement method and the characterization of the proposed elementary cell are discussed in Section IV. Finally, conclusions are drawn in Section V.

II. AFA CONCEPT & CIRCUIT MODEL

1. Antenna–Filter–Antenna Concept

A schematic representation of an AFA array is shown in Fig. 1. Each AFA module is composed of receive antenna, a non-radiating resonant structure, and a transmit antenna [8–12]. Although the frequency characteristics of the antenna set the
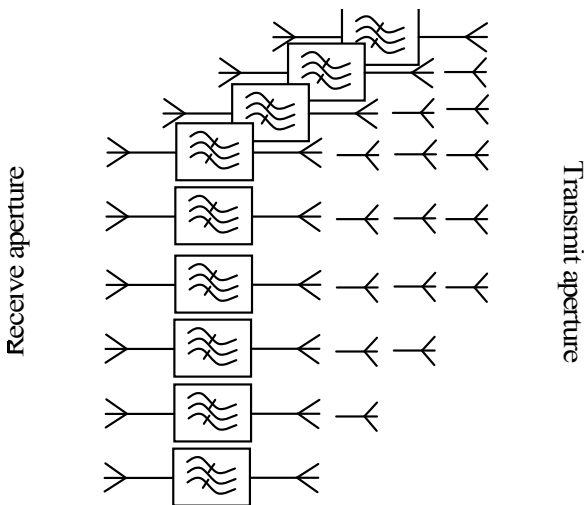

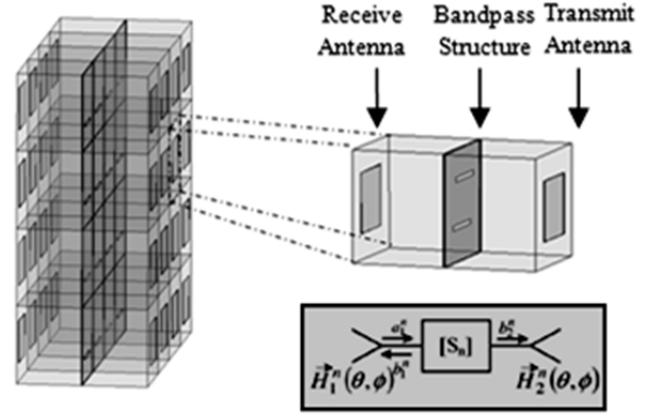Fig. 1. An array of antenna-filter-antenna modules as a bandpass frequency selective surfaces.

Fig. 2. An antenna-filter-antenna array composed of patch antennas and co-planar waveguide resonators.

limit on the transmission bandwidth of these modules, a more general category of filtering shapes can be synthesized using this method. A simple example of such an FSS has been proposed in [6] (based on an earlier work [13]), where a pseudo-highpass filter is formed between the input and output apertures of an array of open ended waveguides.

Fig. 2 shows a case where the radiative elements in the AFA are two back-to-back microstrip patch antennas. The middle resonant structure is an ensemble of CPW resonators fabricated in the common ground plane (referred to as the CPW layer). The coupling between the antennas and the CPW resonators is achieved through coupling slots in the CPW layer. Use of the resonant-type radiative elements is advantageous, since a resonant element by itself can be considered as a combination of a radiative resistance and a resonator. The built-in resonators of the receive/transmit antennas can then be combined with the CPW resonant structure to form a bandpass filter between the radiative ends (see Fig. 3).

For a given filter order, this reduces the required number of the CPW resonators. Special case of the structure is used in [14], where two patch antennas are coupled through a non-resonant slot to form a two-pole bandpass filter. As opposed to the conventional stacked FSS design, a higher order response can be obtained simply by adding resonators in the CPW layer, instead of increasing the number of layers.

2. Antenna–Filter–Antenna Circuit Model

This section describes the general considerations in design of the radiative elements and coupling slots.

The circuit model of the elementary cell is illustrated in Fig. 3. It can be recognized as a band-pass filter. Around the resonant frequency, the antennas are seen as series RLC circuit from the point of view of the resonator. Resistance R_a is proportional to the antenna's radiation resistance, accounting for the losses, and L_a and C_a are the elements representing its resonant behavior.

The resonator is simply modeled as a slot resonator with appropriate length and characteristic impedance. The transformer ratio n is related to the amount of coupling between the patch antennas and the resonator. The value of this coupling allows us to determinate some important filter parameters such as bandwidth and in-band insertion loss, and can be easily controlled by only moving the coupling region from the end of the patch antenna.

The parameters in the antenna circuit model can be extracted from the simulation of the antenna and the coupling slot in an infinite structure, or in a periodic array with a cell size of 3.6 mm which is determined from the effective radiative aperture of the antennas [15]. The critical design parameter, after fixing the antenna and the slot line dimensions, is the value of coupling between the antennas and the resonator. This is controlled by the position of the coupling slot relative to the center of the patch. The proposed circuit model is only valid for a normal incident wave with the electric field polarized parallel to the slot resonator.

According to the circuit model shown in Fig. 3, the input/output coupling of the unit cell is related to the external Q (Q_{ext}) of the end resonators [16]. For a resonant patch element this can be written as [17]:

$$Q_{ext} = Q_r = 2\pi f_0 \frac{W}{P_r} \qquad (1)$$

where f_0 is the resonant frequency, W is the total stored electromagnetic energy, and P_r is the radiated power. Neglecting the losses in the antenna, Q_{ext} can be written in the following form:

$$Q_{ext} = 2\pi f_0 \frac{L_a}{R_a} \qquad (2)$$

where L_a and R_a come from the series RLC model of the antenna (see Fig. 3). In the case of patch antennas, the substrate thickness is particularly important in achieving the desired value of Q_{ext}: the thicker the substrate, the lower Q_{ext} and the wider the passband.

All components of this model are calculated using analytical expressions taking into account the physical parameters of the structure [2].
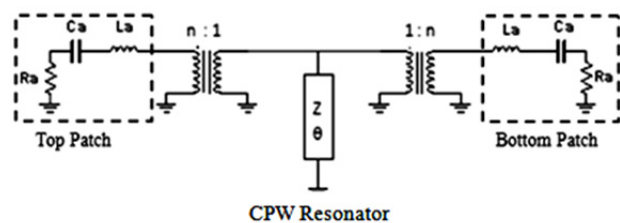
Fig. 3. Circuit model of the antenna-filter-antenna element.

III. AFA Design

The elementary cell, illustrated in Fig. 4, consists of a single ground plane, two substrate layers (Rogers RT/duroid 5880, ε_r = 2.2, $\tan\delta$ = 0.0009, thickness 315 μm) and two patch antennas coupled by a CPW line (2 slots) in the ground plane. This cell can be used in uniform array structures for FSS applications (radome of aircraft), and can also be used in non-uniform array structures for TA applications (e.g., satellite applications). The patch and cell sizes are 1.95 mm × 1.95 mm and 3.6 mm × 3.6 mm ($\lambda_0/2 \times \lambda_0/2$), respectively.

The linear line slot in the ground plane is designed for a good matching for 42 GHz, which corresponds to wavelength in the
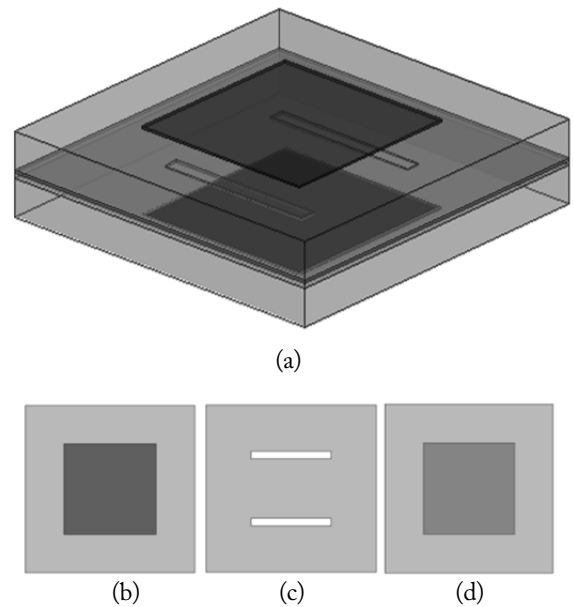
Fig. 4. An antenna-filter-antenna element based on patch antennas and slot resonator. (a) 3D structure, (b) top layer, (c) middle layer, and (d) bottom layer.
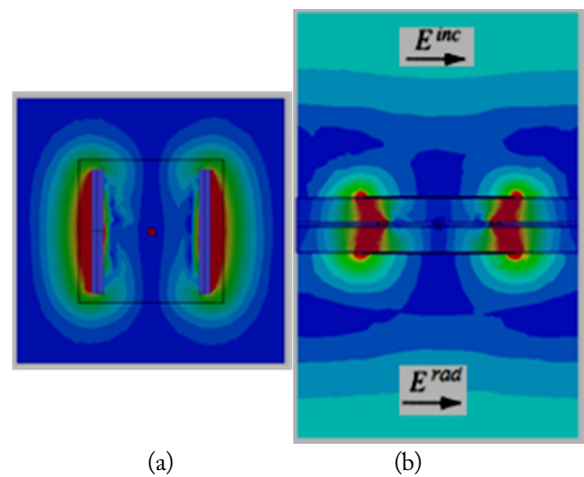
Fig. 5. Passing propagation through the antenna-filter-antenna element. (a) Top view and (b) front view.

substrate λ_g. Consequently, the line slot size is 1.7 mm × 0.16 mm. This elementary cell is a single polarization design. An incident wave with the appropriate polarization is received by the first patch antenna in the input side, passes through the CPW resonator, and reradiates from the second patch antenna with the same polarization, as shown in Fig. 5.

Design and optimization of the element is relatively straightforward and converges after a handful of iterations, by hand-waving between circuit and finite-elements models.

IV. AFA CHARACTERIZATION

The elementary cell was designed with ANSYS-HFSS electromagnetic simulation software using Floquet ports and periodic boundary conditions.

To provide an adequate characterization of the proposed cell we adopted a modified version of the Gaussian quasi-optical measurement systems GOMS [18].

GOMS uses a free space measurement setup that simulates the guided system. Quasi-optical measurement systems have been used for this purpose by a number of researchers [18] for performing similar measurements at 60–300 GHz. However, the required lens/mirror size and focal length prove impractical at Q-band.

Based on the hard-horn developed by Ali et al. [19], a guided measurement system can be developed to simulate an oversized parallel-plate waveguide. Hard-horns are antennas with nearly uniform aperture distribution, which are formed by dielectric loading of the metallic pyramidal horns. A specially designed dielectric lens is used at the aperture to compensate the spherical phase error across the aperture. The hard-horns act as a matched transition between the coaxial terminals and the oversized TEM waveguide ports. The sample under test can be sandwiched between two of these waveguide ports, to form a guided system with coaxial ports.

This system has been successfully used for excitation and measurement of Ka-band quasi-optical amplifier arrays [20]. In our application it is impractical to sandwich the FSS sample between the two hard-horns due to the loading effect of the dielectric lenses. Yet, the hard-horns can be used to form a quasi-guided system.

Fig. 6 shows an antenna array (FLA) in a Gaussian optics measurement system. An input axial beam of the waist radius ω_{01} is generated using a transmit horn antenna. The waist of the input beam is located near the phase-center of the horn and at a distance z_1 from the center of the ARA. The output is a Gaussian beam with the waist of radius ω_{02} at a distance z_2 from the center of the ARA. An open-ended waveguide antenna is used to probe the output radiation intensity along this axis. References [21, 22] give more details about the analytical formulae
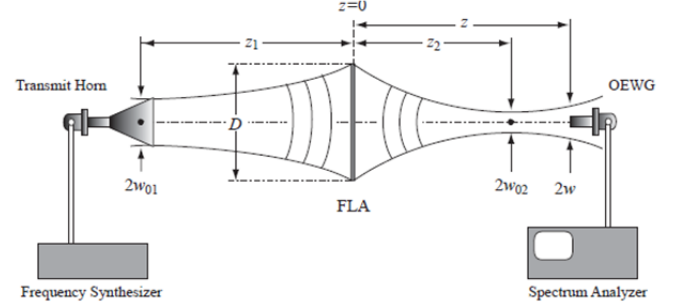

Fig. 6. Antenna under test (FLA) in a Gaussian optics measurement system [21].
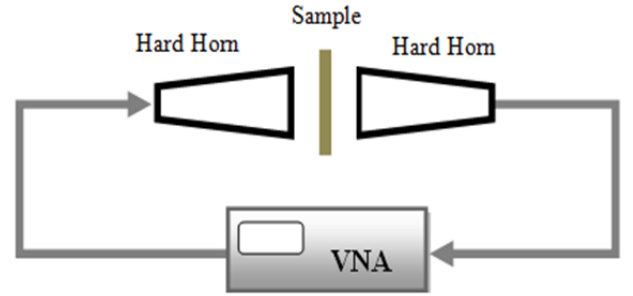

Fig. 7. The free-space measurement system using hard horns.

used to find the different parameters of the measurement setup shown in the Fig. 6.

In our modified system, which is shown in Fig. 7, the hard horns form two parallel TEM ports that are separated by an air gap, and the sample under test is placed in the middle of two ports. Due to their high directivity, the hard-horns are expected to generate a good approximation of the plane wave in the near-field, as is required for the FSS/TA measurements. As the sample can be freely reoriented in the air gap, the quasi-guided system proves convenient for performing measurements at arbitrary angles of the incidence. However, the oblique incidence measurement generally requires larger samples and a wider air gap.

Since the electromagnetic field in the gap region is assumed to be predominantly TEM, the air gaps between the hard horn apertures and the surface of the sample can be treated as transmission-line sections. This allows for a standard thru-reflect-line (TRL) calibration of the measurement setup, which simultaneously de-embeds the connecting cables, hard-horns, and air gaps, from the measurement [22]. Also a time-gating process is applied to filter out the residual error due to the multiple reflections of the high-order modes.

The measurement setup is based on Agilent 8510C vector network analyzer and the hard horns. The hard horns are used as transitions between coaxial input/output and planar wave fronts. A TRL calibration is applied to eliminate the effects of cables, connectors, hard horns, and the air gap between the hard horn apertures and the FSS samples.

The simulated and measured S-parameters under normal incidence are shown in Fig. 8. These results reflect a very good agreement between simulations and experiments. The measurement results show a 27.6% 3-dB bandwidth for 40.5 GHz (18.5% 10-dB).

The maximum in-band insertion loss for this design is <0.2 dB.

Fig. 9 shows the variation in the transmission phase of the AFA element. The phase difference in the 10-dB bandwidth is 132°.

Fig. 10 depicts the computed radiation pattern of the AFA element at 42 GHz. It shows a maximum gain of 4.9 dBi and a 3-dB beamwidth of 86° in E-plane.

The coupling determines the filter's bandwidth and in-band ripple, and can be controlled by changing the exposed distance between the two slots in the ground (W). Table 1 summarizes the matching performance.

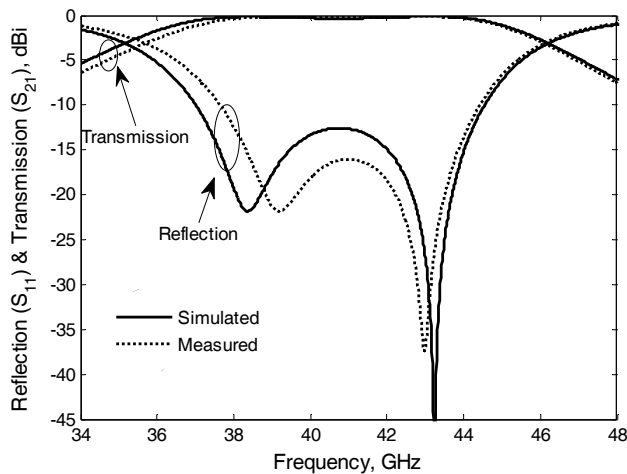The designed unit cell is the first step of a future unit cell design for transmit-arrays. In the case of transmit-array, the main design challenge is the ability to generate the appropriate phase-shift for each cell in order to transform the incoming spherical wave on the free-space side (i.e. to produce a nearly-flat phase distribution or a given phase gradient depending on the main beam direction). Since this phase compensation cannot be ideal, we have previously investigated the effect of phase quantization on the directivity and gain of an array designed in X-band [4]. We have shown that a 1-bit (180° phase steps) and 2-bit (90° phase steps) design result in 4.3 dB and 0.8 dB loss, respectively, compared to the ideal case (Table 2).

Fig. 10. The radiation pattern of the antenna-filter-antenna element at 42 GHz.

Table 1. Matching performance of the elementary cell computed at 42 GHz

Distance between the slots (W of the CPW line) mm	−3 dB bandwidth %	In-band insertion loss dB
2×0.65	30.9	0.8
2×0.70	28.6	0.6
2×0.72	**27.6**	**0.2**
2×0.75	25.9	0.17
2×0.80	23.2	0.1

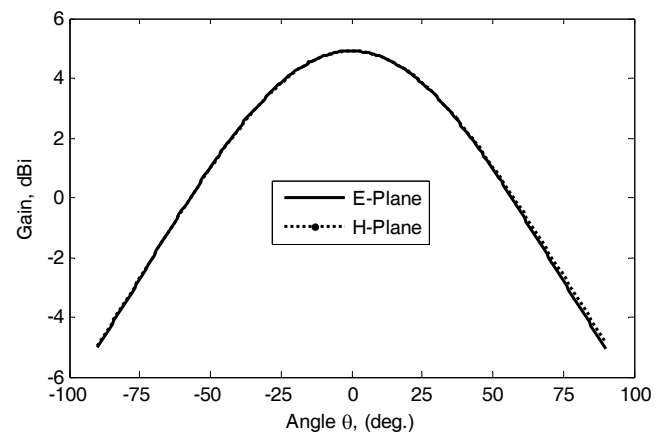
Fig. 8. S-parameters of the antenna-filter-antenna element: measurements vs. simulation.

Fig. 9. Transmission phase of the antenna-filter-antenna element (simulation results).

Table 2. Impact of the phase quantization, transmit-array in X-band [4]

Bit resolution	0-bit	1-bit	2-bit	3-bit	**Ideal**
Directivity (dB)	15.2	25.9	29.4	30	**30.2**
Gain (dB)	12.1	22.8	26.3	26.9	**27.1**

Table 3. Impact of the skew incidence

Incidence θ	0°	10°	20°	30°	40°	**Impact**
$|S_{21}|$	<u>0.95</u>	0.95	0.95	0.94	<u>0.91</u>	**0.04**
Phase (S_{21})	<u>120°</u>	123°	127°	132°	<u>137°</u>	**17°**

Fig. 11. Aircraft, weather radar antenna (transmit-array) under a radome (frequency selective surface).

The effect of the skew incidence on the transmission performances of the proposed elementary cell has been investigated, and was found rather negligible (Table 3). It is worth mentioning that this impact can also be neglected in the case of transmit-array with phase quantization up to 3-bit; as the phase error in that case would be ±22.5° which is larger than the maximum impact of 17° shown in Table 3.

The designed AFA element (FSS) and the future detuned cell (TA) can be used together in the same application; FSS for radome and TA for radar antenna, as illustrated in Fig. 11.

V. CONCLUSION

A simply-structured wideband AFA element has been designed using patch antennas and CPW resonator. A uniform array of these elements exhibits a low loss and sharp roll-off frequency response, which makes it an excellent candidate for filtering application in quasi-optical amplifier arrays and grid mixers. This AFA element has been adequately characterized in non-anechoic environments by using a modified Gaussian optics measurement system. Attractive features, in terms of bandwidth and efficiency, have been achieved by the proposed design. The designed unit cell is the first step of a future unit cell design for lens-arrays and beam-steering for high-speed wireless communication.

REFERENCES

[1] H. Kaouach, L. Dussopt, R. Sauleau, and T. Koleck, "Design and demonstration of an X-band transmit-array," in *Proceedings of 3rd European Conference on Antennas and Propagation (EuCAP)*, Berlin, Germany, 2009, pp. 1191–1195.

[2] H. Kaouach, L. Dussopt, J. Lantéri, T. Koleck, and R. Sauleau, "Wideband low-loss linear and circular polarization transmit-arrays in V-band," *IEEE Transactions on Antennas and Propagation*, vol. 59, no. 7, pp. 2513–2523, 2011.

[3] R. M. S. Cruz, A. G. Assuncao, and P. H. F. da Silva, "A new FSS design proposal for UWB applications," in *Proceedings of 2010 International Workshop on Antenna Technology (iWAT)*, Lisbon, Portugal, 2010, pp. 1–4.

[4] H. Kaouach, L. Dussopt, R. Sauleau, and T. Koleck, "Design and demonstration of 1-bit and 2-bits transmit-array at X-band frequencies," in *Proceedings of 39th European Microwave Conference (EuMC)*, Rome, Italy, 2009, pp. 918–921.

[5] M. P. DeLisio and R. A. York, "Quasi-optical and spatial power combining," *IEEE Transactions on Microwave Theory and Techniques*, vol. 50, no. 3, pp. 929–936, 2002.

[6] B. A. Munk, *Frequency Selective Surfaces*. New York, NY: John Wiley & Sons, 2000.

[7] T. K. Wu, *Frequency Selectives Surfaces and Grid Arrays*. New York, NY: John Wiley & Sons, 1995.

[8] A. Abbaspour-Tamijani, K. Sarabandi, and G. M. Rebeiz, "Antenna-filter-antenna arrays as a class of bandpass frequency-selective surfaces," *IEEE Transactions on Microwave Theory and Techniques*, vol. 52, no. 8, pp. 1781–1789, 2004.

[9] C. C. Cheng and A. Abbaspour-Tamijani, "Study of 2-bit antenna–filter–antenna elements for reconfigurable millimeter-wave lens arrays," *IEEE Transactions on Microwave Theory and Techniques*, vol. 54, no. 12, pp. 4498–4506, 2006.

[10] S. Iyer, C. C. Cheng, C. Kim, and A. Abbaspour-Tamijani, "Compact Gaussian beam system for S-parameter characterization of planar structures at millimeter-wave frequencies," *IEEE Transactions on Instrumentation and Measurement*, vol. 59, no. 9, pp. 2437–2444, 2010.

[11] Y. Li, L. Li, Y. Zhang, and C. Zhao, "Design and synthesis of multilayer frequency selective surface based on antenna-filter-antenna using Minkowski fractal structures," *IEEE Transactions on Antennas and Propagation*, vol. 63, no. 1, pp. 133–141, 2015.

[12] L. Boccia, I. Russo, G. Amendola, and G. Di Massa, "Multilayer antenna-filter antenna for beam-steering transmit-array applications," *IEEE Transactions on Microwave Theory and Techniques*, vol. 60, no. 7, pp. 2287–2300, 2012.

[13] C. J. Larson, "Modified center layer metallic bipolar radome design," Electro Science Lab., Ohio State Univ, Columbus, OH, Tech. Rep. ASAL-TR-78-28, 1978.

[14] R. Pous and D. M. Pozar, "A frequency-selective surface

JOURNAL OF ELECTROMAGNETIC ENGINEERING AND SCIENCE, VOL. 15, NO. 4, OCT. 2015

using aperture couples microtrip patches," *IEEE Transactions on Antennas and Propagation*, vol. 39, no 12, pp. 1763–1769, 1991.

[15] R. Garg, P. Bhartia, I. Bahl, and A. Ittipiboon, *Microstrip Antenna Design Handbook*. Boston, MA: Artech House, 2001.

[16] G. L. Matthaei, L. Young, and E. M. T. Jones, *Microwave Filters, Impedance–Matching Networks and Coupling Structures*. New York, NY: McGraw-Hill, 1964.

[17] R. S. Elliott, *Antenna Theory and Design* (revised ed.). New York, NY: John Wiley & Sons, 2003.

[18] B. C. Deckman, "Active quasi-optics and measurements," Ph.D. dissertation, California Institute of Technology, Pasadena, CA, 2000.

[19] M. A. Ali, S. C. Ortiz, T. Ivanov, and A. Mortazawi, "Analysis and measurement of hard-horn feeds for the excitation of quasi-optical amplifiers," *IEEE Transactions on Microwave Theory and Techniques*, vol. 47, no. 4, pp. 479–487, 1999.

[20] S. C. Ortiz, J. Hubert, L. Mirth, E. Schlecht, and A. Mortazawi, "A high-power Ka-band quasi-optical amplifier array," *IEEE Transactions on Microwave Theory and Techniques*, vol. 50, no. 2, pp. 487–494, 2002.

[21] A. Abbaspour-Tamijani, "Novel components for integrated millimeter-wave front-ends," Ph.D. dissertation, The University of Michigan, Ann Arbor, MI, 2004.

[22] G. F. Engen and C. A. Hoer, "Thru-reflect-line: an improved technique for calibrating the dual six-port automatic network analyzer," *IEEE Transactions on Microwave Theory and Techniques*, vol. 27, no. 12, pp. 987–993, 1979.

Hamza Kaouach

received the M.S. degree in high frequency communications systems from the University of Paris-Est Marne-la-Vallée, France, in 2006 and the Ph.D. degree in signal processing and telecommunications from the University of Rennes 1, France, in 2009. From 2006 to 2009, he was a Research Engineer at CEA-Léti, Grenoble, France. From 2010 to 2012, he was an Antenna and RF Engineer in industries at MATIS Group and PSA Peugeot Citroën Group, Paris, France. Since July 2012, he is an Assistant Professor at the Umm Al-Qura University, College of Enginee-ring at Al-Lith (CEL), ECE Department, Makkah, Saudi Arabia. His current research interests include numerical modeling (FDTD), frequency selective surfaces, measurement antennas, quasi-optic reconfigurable antennas, antenna arrays and transmit arrays at millimeter-wave frequencies. He is a member of the AASCIT and the IEEE.

Amar Kabashi

obtained his M.Sc. and Ph.D. degrees in Electronic & Electrical Engineering from the University of Leeds (UK) in 2007 & 2012, respectively. He has led a mixed professional-research-academic career which brought him right to the crossroads where operators, vendors, regulators, policy makers and international standardization bodies collaborate to shape the future of ICTs. He maintains an active research profile in wireless communications systems and networks. His research interests span a broad spectrum including efficient deployment strategies of hybrid wireless access networks, delay-tolerant and connectivity-challenged ad-hoc and sensor networks, low complexity detection algorithms for multi-carrier systems and telecom network economics and regulation. He is a member of the IET and the IEEE. He is currently holding the position of Assistant Professor of Communication Systems at Umm Al-Qura University, KSA.

Mohammed Talal Simsim

(SM IEEE'12) is associate professor at the department of Electrical Engineering (EE), faculty of Engineering and Islamic Architecture at Umm Al-Qura University (UQU), Makkah, Saudi Arabia. He received the MSc in Electrical Engineering from Colorado State University (CSU) in Fort Collins, CO, USA in 2002 and the Ph.D. in Communications Engineering from UNSW, Sydney, Australia in 2007. He served in several administrative positions at UQU, he is the founder and ex-dean of the College of Engineering – AlLith campus (2011−2013), head of the EE department (2007−2011), founder and ex-director of the Innovation Centre (2011), and vice dean of the Information Technology deanship (2010), all at UQU. He also served as the vice chairman of the Industrial committee in Makkah chamber of commerce during 2009−2011. He served as consultant for the Ministry of Hajj, Saudi Arabia (2011−2012). He is involved in research activities related to academic development, Telecommunications industry, and ICT. He is the chairman of the Innovation consultancy firm, UQU. Since 2013, he is serving as advisor to His Excellency the Minister of Hajj and starting from January 2014, He is supervising Development, Planning, and Consultation Studies at the Ministry of Hajj. Since July 2015, He is the vice-Minister of Hajj.

212